Liu *et al. Chem Synth* 2024;4:10
DOI: 10.20517/cs.2023.51

Chemical Synthesis

Research Article

Open Access

Facile synthesis of heteroporous covalent organic frameworks with dual linkages: a "three-in-one" strategy

Le Liu[1], Xi Su[1], Meiling Qi[1], Xinyue Gao[2], Hao Ren[2,*], Long Chen[1,*]

[1]State Key Laboratory of Supramolecular Structure and Materials, College of Chemistry, Jilin University, Changchun 130012, Jilin, China.
[2]State Key Laboratory of Inorganic Synthesis and Preparative Chemistry, College of Chemistry, Jilin University, Changchun 130012, Jilin, China.

[*]**Correspondence to:** Prof. Long Chen, State Key Laboratory of Supramolecular Structure and Materials, College of Chemistry, Jilin University, 2699 Qianjin Street, Changchun 130012, Jilin, China. E-mail: longchen@jlu.edu.cn; Prof. Hao Ren, State Key Laboratory of Inorganic Synthesis and Preparative Chemistry, College of Chemistry, Jilin University, 2699 Qianjin Street, Changchun, 130012, China. E-mail: renhao@jlu.edu.cn

How to cite this article: Liu L, Su X, Qi M, Gao X, Ren H, Chen L. Facile synthesis of heteroporous covalent organic frameworks with dual linkages: a "three-in-one" strategy. *Chem Synth* 2024;4:10. https://dx.doi.org/10.20517/cs.2023.51

Received: 13 Oct 2023 **First Decision:** 13 Dec 2023 **Revised:** 24 Dec 2023 **Accepted:** 3 Jan 2024 **Published:** 15 Jan 2024

Academic Editors: Li-Hua Chen, Feng Shi **Copy Editor:** Dong-Li Li **Production Editor:** Dong-Li Li

Abstract

Covalent organic frameworks (COFs) with dual linkages can combine advantages and properties of two distinct connectors, enabling the development of multifunctional materials. However, due to challenges in simultaneously forming two types of linkages, the synthesis of COFs with dual linkages remains a significant challenge. Herein, we propose a "three-in-one" molecular design strategy for synthesizing COFs with dual linkages (4-amino-4"-(2,2-dioxan-1,3-dioxan-5-yl)-[1,1':3',1"-terphenyl]-5'-yl) boronic acid (ADTB)-COF and (4'-amino-5'-(4-(2,2-dioxan-1,3-dioxan-5-yl)phenyl)-[1,1':3',1'-teroxan]-5-yl) boronic acid (ADPB)-COF through reversible condensation between three distinct functionalization groups on the monomer. Benefitting from the abundant micropores and high surface area, ADPB-COF showed excellent selective adsorption capability of C_3H_8 over CH_4 (174, 298 K/1 bar). The present work introduces a new approach for constructing COFs with dual linkages, which greatly simplifies the synthesis process and provides a novel opportunity to develop functional materials based on COFs with multi-linkages.

Keywords: Two-dimensional, covalent organic frameworks, dual linkages, light hydrocarbon, adsorption/separation

INTRODUCTION

As a burgeoning crystalline material, covalent organic frameworks (COFs) have exhibited remarkable potentials in diverse fields, including catalysis[1-4], adsorption and separation[5-8], energy storage[9-12], optoelectronic devices[13-15], and sensing[16-19], due to their highly ordered structure, permanent porosity, and excellent stability[20-25]. Since the first example of boroxine-linked COFs reported in 2005[26], COFs with different linkages have been investigated, such as –C=N–[27-29], –C–N–[30-32], –B–O–[33-35], –B–N–[36], –N=N–[37], and –C=C–[38-41]. In this context, the investigation of COFs with dual linkages has garnered significant attention due to their ability to combine the physical and chemical properties from two distinct connectors, thereby endowing COFs with novel functionalities. However, the construction of dual-linkage COFs remains a great challenge due to the presence of multiple functional groups within the framework and possible interference between the formation of two or more covalent bonds, thus complicating the synthesis. Consequently, most reported COFs have been synthesized based on single linkages. Therefore, there is an urgent demand for developing effective and convenient strategies to construct COFs with dual or even multiple linkages.

To achieve the construction of COFs with dual linkages, increasing synthetic efforts have been devoted; however, success has been limited[42-45]. One relatively effective approach is the copolymerization of multi-component monomers, where different functional groups are introduced onto multiple monomers to enable the construction of COFs with various types of covalent bonds. For example, Liang *et al.* reported the construction of dual-linkage dual-pore COFs composed of reversible hydrazone bonds and boroxine rings through the co-condensation of two-component monomers[42]. However, the stoichiometry of different monomers and their distinct solubilities exert a significant impact on the construction of COFs with dual linkages. In most cases, only a part of the monomers were fully dissolved during synthesis. Finding a suitable solvent combination that will dissolve the monomers while maintaining a specific stoichiometry to ensure sufficient 2D or 3D polymerization is a challenge[46]. An alternative strategy involves sequential modulation of reaction conditions to generate diverse covalent bonds for the construction of dual-linkage COFs. For instance, Hu *et al.* reported a new dual-linkage COF (COF-FD1) containing both alkene and imine linkages through orthogonal Schiff base reaction and Knovenagel condensation[44]. However, this approach involves multiple reaction steps, leading to an intricate synthesis of COFs with dual linkages. Considering the above dilemmas, we envisioned that the COFs with dual linkages could be constructed by self-condensation of elaborately designed monomers. In our previous work[47,48], we have developed a "two-in-one" molecular design strategy for the preparation of 2D COFs under simpler conditions. Actually, based on the preparation conditions of COFs, the "three-in-one" strategy to construct COFs with dual linkages by self-condensation of monomers might be an alternate approach to accessing COFs with dual linkages. This strategy not only simplifies the COF synthesis but also improves the solvent adaptability for the monomers, which has, however, not yet been explored.

EXPERIMENTAL

To verify our hypothesis, we designed and synthesized two new trifunctionalized monomers using simple synthetic routes, which were then used to develop COFs with dual linkages ((4-amino-4"-(2,2-dioxan-1,3-dioxan-5-yl)-[1,1':3',1"-terphenyl]-5'-yl)boronic acid (ADTB)-COF and (4'-amino-5'-(4-(2,2-dioxan-1,3-dioxan-5-yl)phenyl)-[1,1':3',1'-teroxan]-5-yl) boronic acid (ADPB)-COF) via the intermolecular self-condensation [Scheme 1]. The corresponding date analysis confirmed that the C=N bond and B_3O_3 ring can be generated simultaneously under solvothermal conditions, demonstrating the successful construction of COFs with dual linkages. In addition, due to the low symmetry of the monomers, the ADTB-COF and ADPB-COF displayed dual pore structures with periodic heterogeneities. Benefiting from the abundant micropores and high surface area, ADPB-COF showed excellent selective adsorption capability of C_3H_8/CH_4

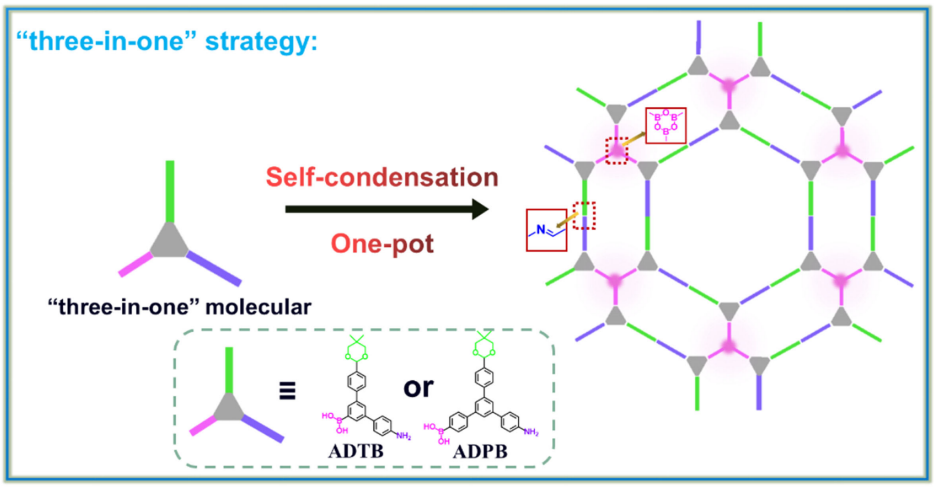

Scheme 1. Schematic diagram of dual-pore 2D COFs with dual linkages constructed by a "three-in-one" strategy. COFs: Covalent organic frameworks; ADTB: (4-amino-4''-(2,2-dioxan-1,3-dioxan-5-yl)-[1,1':3',1''-terphenyl]-5'-yl) boronic acid; ADPB: (4'-amino-5'-(4-(2,2-dioxan-1,3-dioxan-5-yl)phenyl)-[1,1':3',1'-teroxan]-5-yl) boronic acid.

(174, 298 K/1 bar). The current study introduces a novel approach for constructing COFs with dual linkages, which simplified the synthesis process and provided a novel opportunity for developing functional COFs with multiple different linkages.

RESULTS AND DISCUSSION

The new trifunctionalized monomers, ADTB and ADPB [Supplementary Scheme 1], were thoroughly characterized by various methods, including nuclear magnetic resonance spectroscopy and high-resolution mass spectrometry [Supplementary Figures 1-12]. The ADTB-COF and ADPB-COF were synthesized via the self-polycondensation of ADTB and ADPB, respectively, under solvothermal conditions [Supplementary Schemes 2 and 3, Supplementary Figures 13 and 14]. These trifunctionalized modules can be conveniently used to construct dual-linkage COFs in a variety of solvents, unlike most reported COFs, which involved the co-condensation of two or more types of monomers with different functional groups separately. Notably, this strategy could largely avoid the deviation of the stoichiometry between the reaction functional groups, thus highlighting the benefits of this three-in-one strategy.

The as-synthesized ADTB-COF and ADPB-COF were systematically characterized by various techniques. The successful self-condensation of two trifunctionalized monomers has been confirmed by means of Fourier transform infrared spectroscopy [Supplementary Figure 15]. The distinctive vibrations of boric acid groups (≈ 3,578 cm^{-1}), amino groups (≈ 3,372 and ≈ 3,376 cm^{-1}), and aliphatic C–H bonds (≈ 2,845 cm^{-1} and ≈ 2,948 cm^{-1}) in ADTB and ADPB monomers disappeared in the resulting COFs. Furthermore, the distinctive bands of the C=N unit and the B_3O_3 ring were identified at ≈ 1,620 cm^{-1} and ≈ 730 cm^{-1}, respectively, indicating high polymerization in the obtained dual-linkage COFs. In addition, as shown in Supplementary Figure 16, the characteristic signals that appeared at ca. 159 and 127 ppm could be attributed to the carbon of imine bands and the carbon atoms connected with boroxine rings in the solid state ^{13}C CP/MAS NMR spectra[43], which further confirmed the presence of imine units and boroxine rings in both COFs with dual linkages. On the other hand, Elemental analysis was used to determine the C, H, and N contents of two dual-linkage COFs, which were found to be in agreement with theoretical values. The above results demonstrate the successful construction of the two heteroporous COFs with dual linkages and further validate the effectiveness of the "three-in-one" strategy.

The crystalline structures of ADTB-COF and ADPB-COF have been characterized by the powder X-ray diffraction (PXRD) and high-resolution transmission electron microscopy (HRTEM). The PXRD pattern of ADTB-COF [Figure 1A] shows a distinct diffraction peak at 3.01°, corresponding to the (100) lattice plane, with some weaker diffraction peaks at 5.33°, 8.20°, 11.07°, and 26.34°, which could be assigned to (110), (210), (130), and (001) planes, respectively. The simulated PXRD patterns of ADTB-COF with eclipsed (AA) stacking and periodic heterogeneous pore features using the Materials Studio software match better with the experimental patterns than those with the staggered (AB) stacking or the ABC stacking models [Supplementary Figure 17 and Supplementary Table 1][49]. The Pawley refinement based on experimental PXRD patterns revealed the unite cell parameters of $a = b = 34.18$ Å and $c = 3.39$ Å with the *P6*/*M* space group ($R_p = 2.00\%$, $R_{wp} = 2.83\%$) [Figure 1B and C]. HRTEM images showed distinct lattice fringes of the (100) planes with $d_{100} = 29.0$ Å, in good agreement with the structure having the AA stacking heteroporous topology. [Figure 2A and B]. The heteroporous topology of ADPB-COF was analogous to that of ADTB-COF and displayed strong PXRD peaks at 2.45°, 4.67°, 8.10°, and 9.31°, which could be indexed to (100), (200), (220), and (400) planes, respectively. The crystal structure of ADPB-COF was also in good agreement with the AA stacking manner (space group: *P6*/*M*, unit cell parameters: $a = b = 42.69$ Å, $c = 3.45$ Å, Figure 1D-F, Supplementary Figure 18 and Supplementary Table 2), and the difference suggests that experimental result matches well with the refined PXRD pattern in the Pawley refinement ($R_p = 2.93\%$ and $R_{wp} = 3.83\%$). Furthermore, the HRTEM images of ADPB-COF also revealed well-defined lattice fringes of the (100) planes with $d_{100} = 36.2$ Å, consistent with the structure having the AA stacking heteroporous topology [Figure 2C and D]. Scanning electron microscope (SEM) images of two COFs with dual linkages revealed resembling spherical morphology [Figure 2E and F]. Thermogravimetric analysis (TGA) was used to evaluate the thermal stability of the two COFs with dual linkages. The findings showed that both ADTB and ADPB retained 95% of their original weight up to 500 °C in an atmosphere of N_2, demonstrating excellent thermostability [Supplementary Figure 19]. Furthermore, the stability of two COFs was evaluated under a 97% relative humidity (RH) environment. As shown in Supplementary Figure 20, the results demonstrated the efficacy of the dual-linkage strategy in enhancing the water resistance of boroxine-based COFs.

The inherent porosity of the two COFs with dual linkages was evaluated by N_2 sorption measurement at 77 K. A Brunauer-Emmett-Teller (BET) surface area of 247 $m^2 \cdot g^{-1}$ for ADTB-COF and 893 $m^2 \cdot g^{-1}$ for ADPB-COF were calculated by analyzing the low-pressure region ($P/P_0 < 0.20$), as shown in Figure 3A and B [Supplementary Figures 21 and 22]. ADTB-COF showed a lower BET surface area, which may be ascribed to the formation of oligomers during the polymerization process that could obstruct ultra-micropores pores[42,43]. The pore size distributions of ADTB-COF and ADPB-COF were estimated to be 2.23 and 2.06 nm, respectively [Figure 3C and D], using the nonlocal density functional theory (NLDFT) method. These calculated values matched with the pore size predicted from the simulated structures (2.29 nm).

Considering the abundant micropores and high surface area of ADPB-COF, the adsorption of light hydrocarbons was assessed[50]. As methane (CH_4), carbon dioxide (CO_2), ethane (C_2H_6), and propane (C_3H_8) constitute the primary constituents of natural gas, the adsorption isotherms of these four gases on ADPB-COF were measured at 298 and 273 K. There are considerable differences in adsorption isotherms for all four gases [Figure 4A and B]. Specifically, the uptakes of CH_4, CO_2, C_2H_6, and C_3H_8 for ADPB-COF were 3.7, 16.2, 25.3, and 44.1 $cm^3 \cdot g^{-1}$ at 298 K and 1.0 bar, respectively. Notably, the C_3H_8 uptake shows a steep initial rise and then flattens with increasing pressure, belonging to typical type I sorption, indicating a high level of interaction between C_3H_8 molecules and ADPB-COF pores. The higher affinity for ADPB-COFs and the increased uptake is due to the greater polarizability of C_3H_8 compared to the other three gases in this study [62.9×10^{25} cm^3 (C_3H_8) > 44.3×10^{25} cm^3 (C_2H_6) > 27.6×10^{25} cm^3 (CO_2)

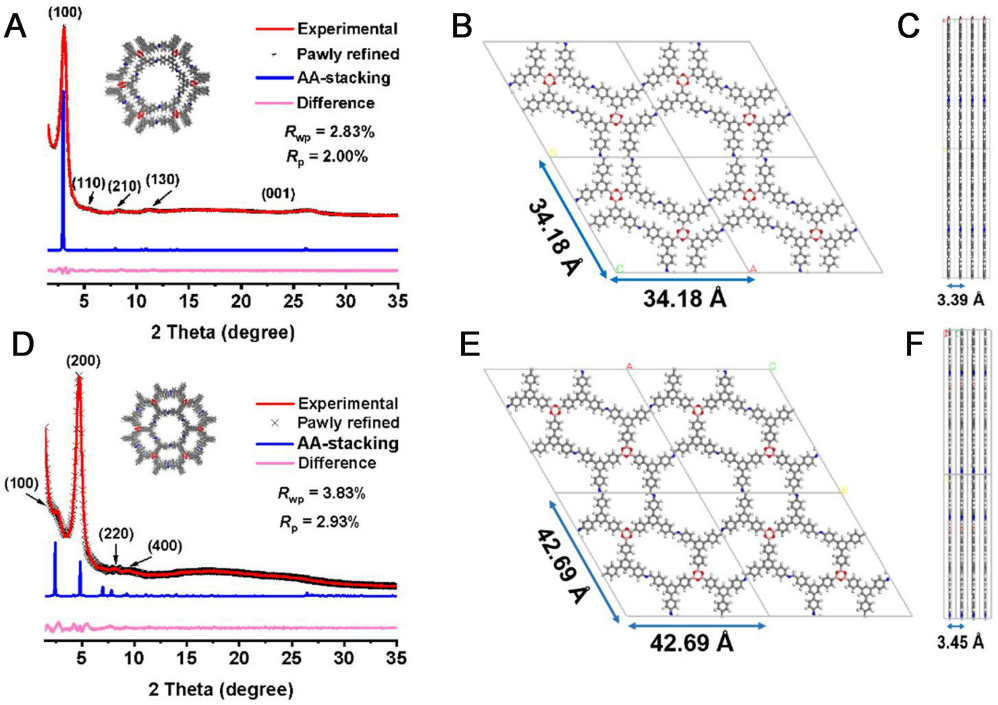

Figure 1. (A) Experimental PXRD patterns (red), refined patterns (black dot), simulated profiles for the eclipsed (AA) stacking model (blue), and the deviation (pink) between experimental and refined patterns of ADTB-COF; (B) Top views and (C) side views of the eclipsed (AA) stacking model for ADTB-COF; (D) Experimental PXRD patterns (red), refined patterns (black dot), simulated profiles for the eclipsed (AA) model (blue), and the deviation (pink) between experimental and refined patterns of ADPB-COF; (E) Top views and (F) side views of the eclipsed (AA) stacking model for ADPB-COF. PXRD: Powder X-ray diffraction; COF: covalent organic framework; ADTB: (4-amino-4"-(2,2-dioxan-1,3-dioxan-5-yl)-[1,1':3',1"-terphenyl]-5'-yl) boronic acid; ADPB: (4'-amino-5'-(4-(2,2-dioxan-1,3-dioxan-5-yl)phenyl)-[1,1':3',1'-teroxan]-5-yl) boronic acid.

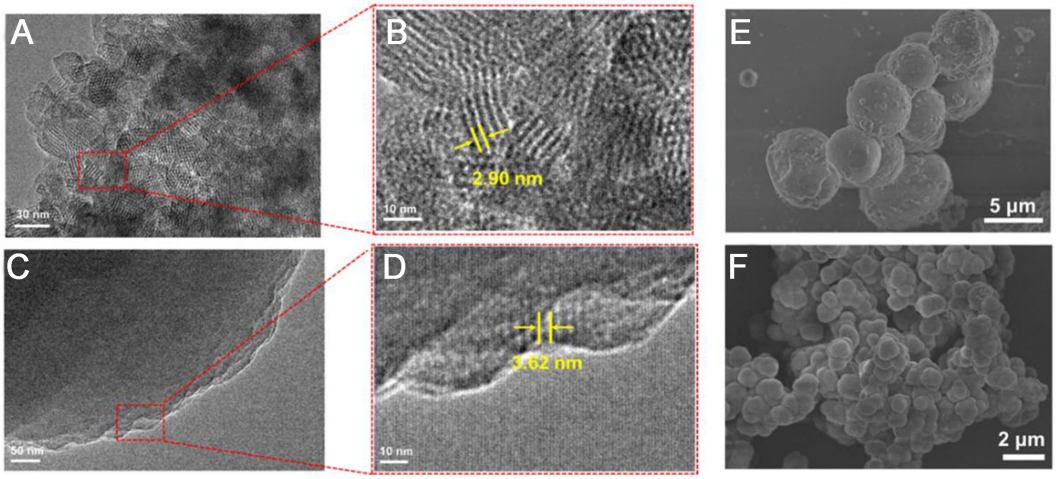

Figure 2. TEM images for (A and B) ADTB-COF and (C and D) ADPB-COF; SEM images for (E) ADTB-COF and (F) ADPB-COF. TEM: Transmission electron microscopy; ADTB: (4-amino-4"-(2,2-dioxan-1,3-dioxan-5-yl)-[1,1':3',1"-terphenyl]-5'-yl) boronic acid; COF: covalent organic framework; ADPB: (4'-amino-5'-(4-(2,2-dioxan-1,3-dioxan-5-yl)phenyl)-[1,1':3',1'-teroxan]-5-yl) boronic acid; SEM: scanning electron microscopy.

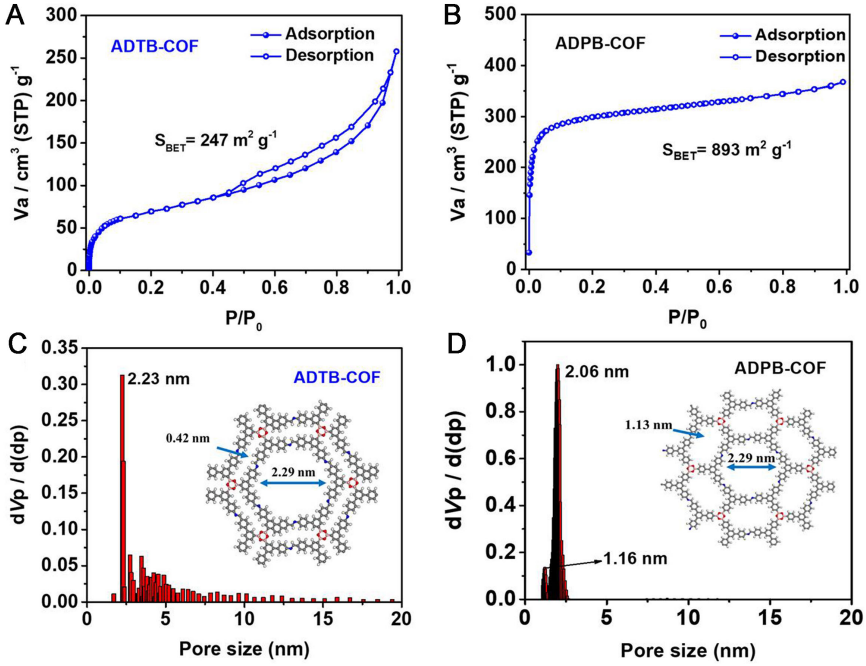

Figure 3. Nitrogen adsorption and desorption isotherms at 77 K of (A) ADTB-COF and (B) ADPB-COF; Pore size distribution by NLDFT of ADTB-COF (C) and (D) ADPB-COF. ADTB: (4-amino-4''-(2,2-dioxan-1,3-dioxan-5-yl)-[1,1':3',1''-terphenyl]-5'-yl) boronic acid; COF: covalent organic framework; ADPB: (4'-amino-5'-(4-(2,2-dioxan-1,3-dioxan-5-yl)phenyl)-[1,1':3',1'-teroxan]-5-yl) boronic acid; NLDFT: nonlocal density functional theory.

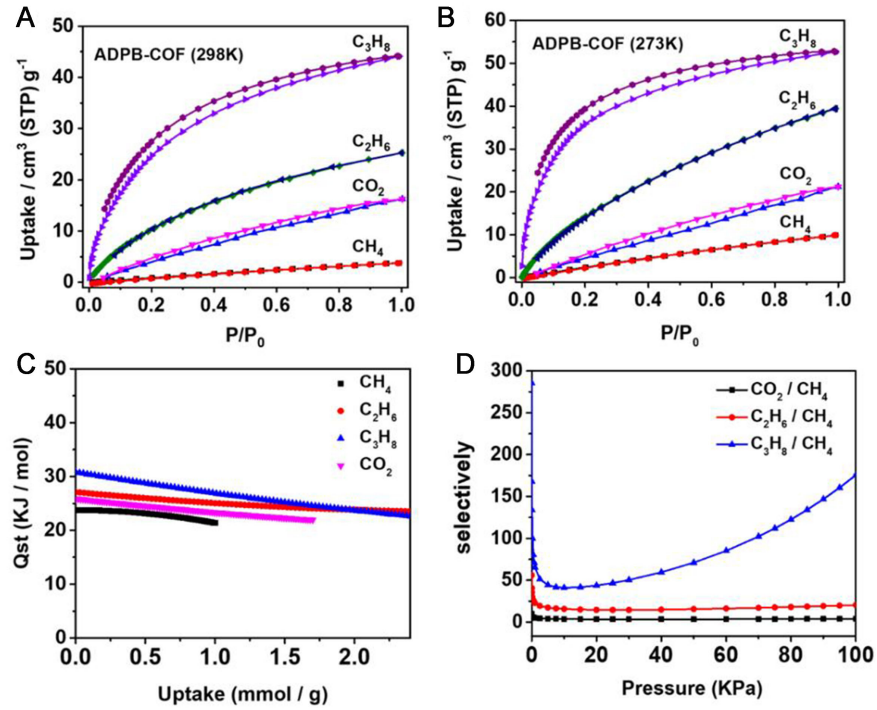

Figure 4. Sorption isotherms for CH_4, CO_2, C_2H_6, and C_3H_8 of ADPB-COF at (A) 298 K and (B) 273 K; (C) Calculated isosteric heats of CH_4, CO_2, C_2H_6, and C_3H_8 on ADPB-COF and (D) IAST calculations for adsorption selectivity of equimolar CO_2/CH_4, C_2H_6/CH_4, and C_3H_8/CH_4 gas mixtures on ADPB-COF at 298 K. ADPB: (4'-amino-5'-(4-(2,2-dioxan-1,3-dioxan-5-yl)phenyl)-[1,1':3',1'-teroxan]-5-yl) boronic acid; COF: covalent organic framework; IAST: ideal adsorption solution theory.

> 25.9 × 10^{25} cm^3 (CH_4)][51]. Consequently, the C_3H_8 is more susceptible to polarization by the framework, resulting in the formation of an induced dipole and an increase in adsorption capacity. Notably, among these gases, C_3H_8 exhibits the highest critical temperature [369.8 K (C_3H_8) > 305.4 K (C_2H_6) > 304.2 K (CO_2) > 190.6 K (CH_4)][52], making it easily condensable and adsorbable on the porous surfaces.

Furthermore, as shown in Figure 4C, the isosteric heat was used to evaluate the adsorption affinity between CH_4/CO_2/C_2H_6/C_3H_8 and ADPB-COF. The isosteric heats of ADPB-COF for C_3H_8, C_2H_6, CO_2, and CH_4 are 30.8, 27.3, 25.8, and 23.6 kJ/mol, respectively. Therefore, the steepness of the initial gas uptake and the adsorption capacity of the four gases follow a descending trend in the order (C_3H_8 > C_2H_6 > CO_2 > CH_4), which can also be attributed to their distinct physicochemical properties. The significant difference in isosteric heat among CH_4, CO_2, C_2H_6, and C_3H_8 on ADPB-COF also indicates the high potential for separating light hydrocarbons.

Furthermore, the selectivity of binary components with an equal molar ratio was assessed using the ideal adsorption solution theory (IAST). The models were constructed with high precision (R^2 > 0.999) to accurately fit the experimental single-component isotherms at 298 K and 1.0 bar through the single site Langmuir-Freundlich equation [Supplementary Figures 23-26 and Supplementary Table 3]. The gas mixtures of C_3H_8/CH_4, C_2H_6/CH_4, and CO_2/CH_4 were set at a ratio of 1:1, and the selectivities obtained were plotted as a function of the mixed gas pressure, ranging from 0 to 1.0 bar. As shown in Figure 4D, ADPB-COF showed excellent selectivity for the mixtures of C_3H_8 and CH_4 at 298 K and 1.0 bar, with a selectivity as high as 174 (4 for CO_2/CH_4, 20 for C_2H_6/CH_4). Compared with other representative porous materials based on the separation of C_3H_8/CH_4 [Supplementary Table 4], ADPB-COF featured a favorable selectivity. These results indicate that the dual-linkage COF materials may exhibit superior performance in methane separation from natural gas, thereby offering a new approach for light hydrocarbon purification.

CONCLUSIONS

In conclusion, we propose a new "three-in-one" strategy for synthesizing heteroporous 2D COFs with dual linkages (ADTB-COF and ADPB-COF) through self-polycondensation of two trifunctionalized simplex monomers, respectively. Benefitting from the abundant micropores and high surface area, ADPB-COF showed excellent selectivity of C_3H_8 over CH_4 (174, 298 K/1 bar). The current study introduced a novel approach for constructing COFs with dual linkages, which greatly simplified the synthetic process and provided a new opportunity for developing functional COFs with multiple different linkages.

DECLARATIONS

Authors' contributions

Designed the topic and provided ideas: Chen L
Collected the data, provided administrative, technical, and material support, and drafted the manuscript: Liu L, Su X, Qi M, Gao X, Ren H

Availability of data and materials

Not applicable.

Financial support and sponsorship

This work was financially supported by the National Natural Science Foundation of China (51973153 and 21975096).

Conflicts of interest

All authors declared that there are no conflicts of interest.

Ethical approval and consent to participate

Not applicable.

Consent for publication

Not applicable.

REFERENCES

1. Qian C, Zhou W, Qiao J, et al. Linkage engineering by harnessing supramolecular interactions to fabricate 2D hydrazone-linked covalent organic framework platforms toward advanced catalysis. *J Am Chem Soc* 2020;142:18138-49. DOI
2. Song D, Xu W, Li J, et al. "All-in-one" covalent organic framework for photocatalytic CO_2 reduction. *Chinese J Catal* 2022;43:2425-33. DOI
3. Yang Z, Hao W, Su X, et al. Metallosalphen-based 2D covalent organic frameworks with an unprecedented tju topology via K-shaped two-in-one monomers. *Chem Mater* 2022;34:5888-95. DOI
4. Zhao Z, Chen X, Li B, et al. Spatial regulation of acceptor units in olefin-linked COFs toward highly efficient photocatalytic H_2 evolution. *Adv Sci* 2022;9:2203832. DOI PubMed PMC
5. Díaz U, Corma A. Ordered covalent organic frameworks, COFs and PAFs. From preparation to application. *Coord Chem Rev* 2016;311:85-124. DOI
6. Li J, He Y, Zou Y, Yan Y, Song Z, Shi X. Achieving a stable COF with the combination of "flat" and "twist" large-size rigid synthons for selective gas adsorption and separation. *Chin Chem Lett* 2022;33:3017-20. DOI
7. Moroni M, Roldan-Molina E, Vismara R, Galli S, Navarro JAR. Impact of pore flexibility in imine-linked covalent organic frameworks on benzene and cyclohexane adsorption. *ACS Appl Mater Interfaces* 2022;14:40890-901. DOI PubMed PMC
8. Zhao Z, Liang S, Kang C, et al. Reversing adsorption and separation of 1-phenylethanol and acetophenone in organic phase via β-ketoenamine-linked covalent organic frameworks. *Chem Eng J* 2023;454:140531. DOI
9. Tong Y, Sun Z, Wang J, Huang W, Zhang Q. Covalent organic framework containing dual redox centers as an efficient anode in Li-ion batteries. *SmartMat* 2022;3:685-94. DOI
10. Iqbal R, Yasin G, Hamza M, et al. State of the art two-dimensional covalent organic frameworks: prospects from rational design and reactions to applications for advanced energy storage technologies. *Coord Chem Rev* 2021;447:214152. DOI
11. Patra BC, Bhattacharya S. New covalent organic square lattice based on porphyrin and tetraphenyl ethylene building blocks toward high-performance supercapacitive energy storage. *Chem Mater* 2021;33:8512-23. DOI
12. Mohammed AK, Vijayakumar V, Halder A, et al. Weak intermolecular interactions in covalent organic framework-carbon nanofiber based crystalline yet flexible devices. *ACS Appl Mater Interfaces* 2019;11:30828-37. DOI
13. Wang C, Zhang Z, Zhu Y, Yang C, Wu J, Hu W. 2D covalent organic frameworks: from synthetic strategies to advanced optical-electrical-magnetic functionalities. *Adv Mater* 2022;34:2102290. DOI
14. Zhao R, Wang T, Li J, et al. Two-dimensional covalent organic frameworks for electrocatalysis: achievements, challenges, and opportunities. *Nano Res* 2023;16:8570-95. DOI
15. Zhang H, Geng Y, Huang J, Wang Z, Du K, Li H. Charge and mass transport mechanisms in two-dimensional covalent organic frameworks (2D COFs) for electrochemical energy storage devices. *Energy Environ Sci* 2023;16:889-951. DOI
16. Bhunia S, Deo KA, Gaharwar AK. 2D covalent organic frameworks for biomedical applications. *Adv Funct Mater* 2020;30:2002046. DOI
17. Guo L, Yang L, Li M, Kuang L, Song Y, Wang L. Covalent organic frameworks for fluorescent sensing: recent developments and future challenges. *Coord Chem Rev* 2021;440:213957. DOI
18. Jiang S, Meng L, Ma W, et al. Dual-functional two-dimensional covalent organic frameworks for water sensing and harvesting. *Mater Chem Front* 2021;5:4193-201. DOI
19. Tan Z, Wang J, Xu L, et al. Simultaneous sensing of multiplex volatile organic compounds by adsorption and plasmon dual-induced raman enhancement technique. *ACS Sens* 2023;8:867-74. DOI
20. Liang RR, Jiang SY, A RH, Zhao X. Two-dimensional covalent organic frameworks with hierarchical porosity. *Chem Soc Rev* 2020;49:3920-51. DOI PubMed
21. Zhi Y, Wang Z, Zhang HL, Zhang Q. Recent progress in metal-free covalent organic frameworks as heterogeneous catalysts. *Small* 2020;16:2001070. DOI PubMed
22. Li C, Yu G. Controllable synthesis and performance modulation of 2D covalent-organic frameworks. *Small* 2021;17:2100918. DOI

PubMed
23. Zhang T, Zhang G, Chen L. 2D conjugated covalent organic frameworks: defined synthesis and tailor-made functions. *Acc Chem Res* 2022;55:795-808. DOI PubMed
24. Xu J, Xu Y, Bu XH. Advances in emerging crystalline porous materials. *Small* 2021;17:2102331. DOI PubMed
25. Geng K, Arumugam V, Xu H, Gao Y, Jiang D. Covalent organic frameworks: polymer chemistry and functional design. *Prog Polym Sci* 2020;108:101288. DOI
26. Côté AP, Benin AI, Ockwig NW, O'Keeffe M, Matzger AJ, Yaghi OM. Porous, crystalline, covalent organic frameworks. *Science* 2005;310:1166-70. DOI PubMed
27. Romero-Muñiz I, Mavrandonakis A, Albacete P, et al. Unveiling the local structure of palladium loaded into imine-linked layered covalent organic frameworks for cross-coupling catalysis. *Angew Chem Int Ed Engl* 2020;59:13013-20. DOI PubMed
28. Liang B, Zhao J, Wang J, et al. Nonlinear optical properties of porphyrin-based covalent organic frameworks determined by steric-orientation of conjugation. *J Mater Chem C* 2023;11:3354-9. DOI
29. Helweh W, Flanders NC, Wang S, et al. Layered structures of assembled imine-linked macrocycles and two-dimensional covalent organic frameworks give rise to prolonged exciton lifetimes. *J Mater Chem C* 2022;10:3015-26. DOI
30. Das P, Mandal SK. Flexible and semi-flexible amide-hydrazide decorated fluorescent covalent organic frameworks as on-off pH responsive proton scavengers. *ACS Appl Mater Interfaces* 2021;13:14160-8. DOI PubMed
31. Kang J, Hang J, Chen B, et al. Amide linkages in pyrene-based covalent organic frameworks toward efficient photocatalytic reduction of uranyl. *ACS Appl Mater Interfaces* 2022;14:57225-34. DOI
32. Zhou ZB, Han XH, Qi QY, Gan SX, Ma DL, Zhao X. A facile, efficient, and general synthetic method to amide-linked covalent organic frameworks. *J Am Chem Soc* 2022;144:1138-43. DOI
33. Xiao Z, Li L, Tang Y, et al. Covalent organic frameworks with lithiophilic and sulfiphilic dual linkages for cooperative affinity to polysulfides in lithium-sulfur batteries. *Energy Stor Mater* 2018;12:252-9. DOI
34. Castano I, Evans AM, Dos Reis R, Dravid VP, Gianneschi NC, Dichtel WR. Mapping grains, boundaries, and defects in 2D covalent organic framework thin films. *Chem Mater* 2021;33:1341-52. DOI PubMed PMC
35. Hu J, Gupta SK, Ozdemir J, Beyzavi MH. Applications of dynamic covalent chemistry concept towards tailored covalent organic framework nanomaterials: a review. *ACS Appl Nano Mater* 2020;3:6239-69. DOI PubMed PMC
36. Jackson KT, Reich TE, El-Kaderi HM. Targeted synthesis of a porous borazine-linked covalent organic framework. *Chem Commun* 2012;48:8823-5. DOI PubMed
37. Hota MK, Chandra S, Lei Y, et al. Electrochemical thin-film transistors using covalent organic framework channel. *Adv Funct Mater* 2022;32:2201120. DOI
38. Xu X, Zhang S, Xu K, Chen H, Fan X, Huang N. Janus Dione-based conjugated covalent organic frameworks with high conductivity as superior cathode materials. *J Am Chem Soc* 2023;145:1022-30. DOI PubMed
39. Zhao Y, Liang Y, Wu D, et al. Ruthenium complex of sp^2 carbon-conjugated covalent organic frameworks as an efficient electrocatalyst for hydrogen evolution. *Small* 2022;18:2107750. DOI PubMed
40. Cheng YZ, Ji W, Wu X, Ding X, Liu XF, Han BH. Persistent radical cation sp^2 carbon-covalent organic framework for photocatalytic oxidative organic transformations. *Appl Catal B Environ* 2022;306:121110. DOI
41. Yue JY, Ding XL, Wang YT, et al. Dual functional sp^2 carbon-conjugated covalent organic frameworks for fluorescence sensing and effective removal and recovery of Pd^{2+} ions. *J Mater Chem A* 2021;9:26861-6. DOI
42. Liang RR, A RH, Xu SQ, Qi QY, Zhao X. Fabricating organic nanotubes through selective disassembly of two-dimensional covalent organic frameworks. *J Am Chem Soc* 2020;142:70-4. DOI PubMed
43. Zeng Y, Zou R, Luo Z, et al. Covalent organic frameworks formed with two types of covalent bonds based on orthogonal reactions. *J Am Chem Soc* 2015;137:1020-3. DOI
44. Hu J, Zhang J, Lin Z, Xie L, Liao S, Chen X. Construction of a hollow spherical covalent organic framework with olefin and imine dual linkages based on orthogonal reactions. *Chem Mater* 2022;34:5249-57. DOI
45. Xu X, Wu X, Xu K, Xu H, Chen H, Huang N. Pore partition in two-dimensional covalent organic frameworks. *Nat Commun* 2023;14:3360. DOI PubMed PMC
46. Smith BJ, Dichtel WR. Mechanistic studies of two-dimensional covalent organic frameworks rapidly polymerized from initially homogenous conditions. *J Am Chem Soc* 2014;136:8783-9. DOI PubMed
47. Li Y, Chen Q, Xu T, et al. De novo design and facile synthesis of 2D covalent organic frameworks: a two-in-one strategy. *J Am Chem Soc* 2019;141:13822-8. DOI PubMed
48. Li Y, Chen W, Xing G, Jiang D, Chen L. New synthetic strategies toward covalent organic frameworks. *Chem Soc Rev* 2020;49:2852-68. DOI
49. Li Y, Su X, Zheng W, et al. Targeted synthesis of isomeric naphthalene-based 2D kagome covalent organic frameworks. *Angew Chem Int Ed Engl* 2023;62:e202216795. DOI PubMed
50. Li G, Wang Z. Micro- and ultramicroporous polyaminals for highly efficient adsorption/separation of C_1-C_3 hydrocarbons and CO_2 in natural gas. *ACS Appl Mater Interfaces* 2020;12:24488-97. DOI PubMed
51. Zhang S, Taylor MK, Jiang L, Ren H, Zhu G. Light hydrocarbon separations using porous organic framework materials. *Chemistry* 2020;26:3205-21. DOI
52. Li JR, Kuppler RJ, Zhou HC. Selective gas adsorption and separation in metal-organic frameworks. *Chem Soc Rev* 2009;38:1477-504. DOI PubMed